Frequency-dependent squeezing for gravitational wave detection through quantum teleportation

Yohei Nishino[1,2,3*], Stefan Danilishin[3,4], Yutaro Enomoto[5], Teng Zhang[6]

[1*]Department of Astronomy, University of Tokyo, Bunkyo, Tokyo, 113-0033, Japan.
[2]Gravitational Wave Science Project, National Astronomical Observatory of Japan (NAOJ), Mitaka City, Tokyo, 181-8588, Japan.
[3]Department of Gravitational Waves and Fundamental Physics, Maastricht University, 6200 MD, Maastricht, The Netherlands.
[4]Nikhef – National Institute for Subatomic Physics, Science Park 105, 1098 XG Amsterdam, The Netherlands.
[5]Department of Applied Physics, The University of Tokyo, Bunkyo, Tokyo, 113-0033, Japan.
[6]The University of Birmingham, School of Physics and Astronomy, and Institute of Gravitational Wave Astronomy, University of Birmingham, Edgbaston, Birmingham, B15 2TT, United Kingdom.

*Corresponding author(s). E-mail(s): yohei.nishino@grad.nao.ac.jp;
Contributing authors: s.danilishin@nikhef.nl; yenomoto.ap.t@gmail.com; tzhang@star.sr.bham.ac.uk;

Abstract

This is a supplementary information for the paper "Frequency-dependent squeezing for gravitational-wave detection through quantum teleportation"

1 Interferometer response for idlers

In this section, we examine the response of the central interferometer as filter cavities for two idlers. We show the parameter optimization process, crucial for using the

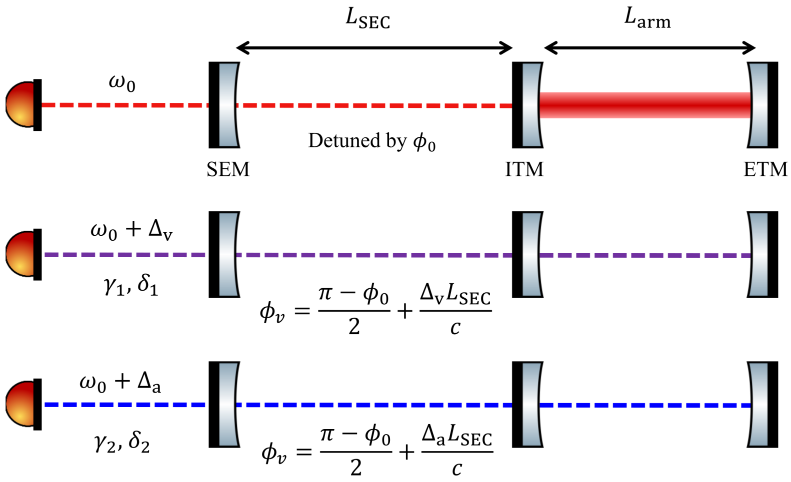

Fig. 1 Resonance conditions for differential mode cavities: Shown from top to bottom are the resonance conditions for Bob, Alice and Victor.

interferometer as quantum filter cavities to our specific requirements, then investigate the effect of the arm cavity and SEC losses onto those filter parameters, comparing the conventional filter cavity scheme.

1.1 Parameter searching

The coupled cavity formed by the SEC, ITM and ETM functions as a passive optical cavity for two idler beams. Due to the phase shifts acquired in the SEC, the bandwidths for two idlers can be tuned to meet the requirement of filter cavity bandwidths. To begin, let's examine the bandwidth of the arm cavity, which can be expressed as:

$$\gamma_{1\mathrm{arm}} = \frac{cT_{\mathrm{ITM}}}{4L_{\mathrm{arm}}} \tag{1}$$

According to the scaling law theorem [1, 2], the effective bandwidth can be expressed as follows:

$$\begin{aligned} \gamma &= \gamma_{1\mathrm{arm}} \mathrm{Re}\left[\frac{1-\sqrt{R_{\mathrm{SEM}}}e^{2i\phi_{\mathrm{SEC}}}}{1+\sqrt{R_{\mathrm{SEM}}}e^{2i\phi_{\mathrm{SEC}}}}\right] \\ &= \frac{\gamma_{1\mathrm{arm}} T_{\mathrm{SEM}}}{1+2\sqrt{R_{\mathrm{SEM}}}\cos 2\phi_{\mathrm{SEC}} + R_{\mathrm{SEM}}}, \end{aligned} \tag{2}$$

leading the requirement of round-trip phase ϕ_{SEC}:

$$\phi_{\mathrm{SEC}} = \frac{1}{2}\left[\arccos\left(\frac{T_{\mathrm{SEM}}\frac{\gamma_{1\mathrm{arm}}}{\gamma} - 1 - R_{\mathrm{SEM}}}{2\sqrt{R_{\mathrm{SEM}}}}\right)\right] + n\pi. \tag{3}$$

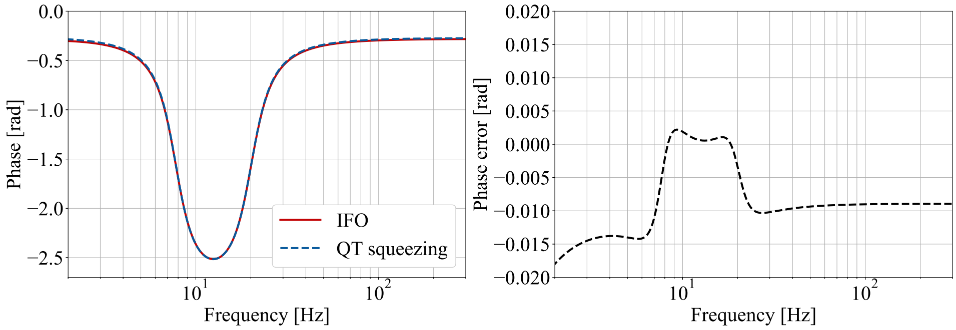

Fig. 2 Left panel: Quadrature rotations. The solid red curve is caused by the interferometer (IFO) and the dashed blue curve is rotation given to two idlers. Right panel: Angle error between the two rotations.

Here, n is an integer that determines the number of spectral ranges of the SEC. The phase $\phi_{\rm SEC}$ for Victor and Alice, denoting as $\phi_{v,a}$, can be described as:

$$\phi_{v,a} = \frac{(\omega_0 + \Delta_{v,a})L_{\rm SEC}}{c} = \frac{\pi - \phi_0}{2} + \frac{\Delta_{v,a}L_{\rm SEC}}{c}, \tag{4}$$

where ϕ_0 represents the detuning phase of the SEC for the main carrier. $\phi_{v,a}$ should be tuned to realize the required filter cavity bandwidth $\gamma_{1,2}$; substituting Eq. (4) into Eq. (3), $\Delta_{v,a}$ need to satisfy the following relation:

$$\Delta_{v,a} = \frac{c}{2L_{\rm SEC}}\left[\arccos\left(\frac{T_{\rm SEM}\frac{\gamma_{\rm 1arm}}{\gamma_{1,2}} - 1 - R_{\rm SEM}}{2\sqrt{R_{\rm SEM}}}\right) + (2n_{v,a} - 1)\pi + \phi_0\right], \tag{5}$$

having $n_{1,2}$ as free parameters. On the other hand, $\phi_{v,a}$ should also satisfy the following relation to realize the effective detunings $\delta_{1,2}$ as:

$$\delta_{1,2} = \mathrm{Mod}_{\omega_{\rm FSR}^{\rm arm}}(\Delta_{v,a}) - \gamma_{\rm 1arm}\mathrm{Im}\left[\frac{1 - \sqrt{R_{\rm SEM}}e^{2i\phi_{v,a}}}{1 + \sqrt{R_{\rm SEM}}e^{2i\phi_{v,a}}}\right], \tag{6}$$

where $\omega_{\rm FSR}^{\rm arm}$ is the FSR of the arm cavity.

We have four tunable parameters: macroscopic arm and SEC length, $\delta L_{\rm arm} = q\lambda/2$ and $\delta L_{\rm SEC} = p\lambda/2$ where q and p are integer values, and $n_{v,a}$ meaning the number of the SEC spectral ranges contained in $\Delta_{v,a}$. In Table 1, we provide the optimal length and frequency tuning parameters. The adjustments required for both the arm and SEC are approximately 1.6 and 2.4 cm, respectively. Detuning frequencies of Victor and Alice are approximately $\Delta_a \sim 32.9$ MHz and $\Delta_v \sim -789$ MHz. Fig 2 illustrates a comparison of phase rotations, highlighting the ponderomotive squeezing and the approximate rotations achieved through the combination of the two idlers.

Parameter List		
λ	Carrier wavelength	1550 nm
T_{arm}	ITM power transmittance	7000 ppm
T_{SEM}	SEM power transmittance	90 %
T_{PCM}	PCM power transmittance	20 %
m	Mirror mass	211 kg
I_0	Power at BS	63 W
ϕ_0	Detuning of the SEC	0.75 rad
$L_{\mathrm{arm}}^{(0)}$	Arm initial length	10 km [1]
$L_{\mathrm{SEC}}^{(0)}$	SEC initial length	100 m
$\gamma_{1\mathrm{arm}}$	Arm cavity bandwidth	8.35 Hz
γ_1/δ_1	bandwidth/detuning of the first FC	4.27/19.54 Hz
γ_2/δ_2	bandwidth/detuning of the second FC	1.64/-7.62 Hz
δL_{arm}	Arm length tuning	10497λ
δL_{SEC}	SEC length tuning	15790λ
Δ_a	Detuning of Alice	$768\ \mathrm{kHz} + 11\ \mathrm{FSR_{SEC}}$ [2]
Δ_v	Detuning of Victor	$655\ \mathrm{kHz} + 1059\ \mathrm{FSR_{SEC}}$

[1]To be more precise, $L_{\mathrm{arm}}^{(0)} = 6451612903\lambda$ and $L_{\mathrm{SEC}}^{(0)} = 64516129\lambda$, where λ is the wavelength of the main laser.

[2]$n_a = 11$ and $n_v = 1059$.

Table 1 Parameters for ETLF [3]

1.2 Effect of arm cavity and SEC loss

The arm cavity loss contains the power loss per each mirror and the transmissivity of the end mirror, which has values of 20 ppm and 5 ppm in the current design of ET. The arm loss is amplified by the arm cavity approximately by a factor of finesse, which expands the bandwidth of the coupled cavity as a filter cavity for idlers. On the other hand, the SEC loss contribution to the cavity bandwidth is not significant even though it has a large value as 1000 ppm.

According to the scaling-law theorem, the effective bandwidth of the lossy SEC-arm coupled cavity, $\gamma_{\mathrm{loss}}^{\mathrm{eff}}$, can be expressed as follows:

$$\begin{aligned} \gamma_{\mathrm{loss}}^{\mathrm{eff}} = \gamma_{\mathrm{loss}} + \gamma_2 &= \frac{(T_{\mathrm{SEC}} + A_{\mathrm{SEC}})\gamma_{1\mathrm{arm}}}{1 + 2\sqrt{R_{\mathrm{SEC}}}\cos 2\phi_{\mathrm{SEC}} + R_{\mathrm{SEC}}} + \frac{cA_{\mathrm{arm}}}{4L_{\mathrm{arm}}} \\ &= \frac{T_S\gamma_{1\mathrm{arm}}}{1 + 2\sqrt{R_{\mathrm{SEC}}}\cos 2\phi_{\mathrm{SEC}} + R_{\mathrm{SEC}}} + \frac{cA^{\mathrm{eff}}}{4L_{\mathrm{arm}}}, \end{aligned} \tag{7}$$

where

$$A^{\mathrm{eff}} = \frac{T_{\mathrm{arm}}A_{\mathrm{SEC}}}{1 + 2\sqrt{R_{\mathrm{SEC}}}\cos 2\phi_{\mathrm{SEC}} + R_{\mathrm{SEC}}} + A_{\mathrm{arm}}. \tag{8}$$

Here, γ_{loss} represents the coupled-cavity bandwidth when arm cavities have no loss, and γ_2 is the contribution of the arm cavity loss to expansion of the bandwidth and ϕ_{SEC} is the one-way phase inside the SEC for idlers. Eq.(8) is the expansion of the bandwidth due to the losses. Using the current ETLF parameter, the numerator of the first term $T_{\mathrm{arm}}A_{\mathrm{SEC}}$ is calculated as 7 ppm. Considering the amplification gains

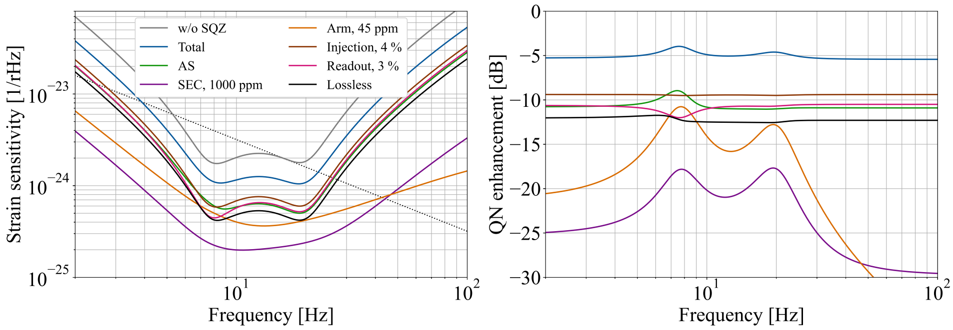

Fig. 3 Left panel: Noise contributions of each loss source to the strain sensitivity. Phase noises such as squeezer noise rms, local oscillator rms, and SEC length rms are all encompassed within the AS noise. The black curve depicts the ideal case without imperfections. Right panel: Quantum noise enhancement factor in dB compared to the noise spectrum without squeezing (shown in gray in the left panel).

by the denominator for two idlers, approximately 1.0 and 2.5 respectively, the effective filter cavity losses are $A_v^{\text{eff}} \sim 52$ ppm and $A_a^{\text{eff}} \sim 63$ ppm. Since the length of the filter cavity is that of the arm cavity $L_{\text{arm}} = 10$ km, the QT squeezing has less noise contribution than conventional filter cavities in terms of the loss per unit length (This is explained also in the references [4, 5]). Given the round-trip loss in the filter cavity is $A_{\text{FC}} = 20$ ppm, and the length $L_{\text{FC}} = 1$ km, discussion above leads:

$$\frac{A_{v,a}^{\text{eff}}}{L_{\text{arm}}} < \frac{A_{\text{FC}}}{L_{\text{FC}}},$$

showing that the optical loss contribution to the expansion of the filter-cavity bandwidth is smaller in the QT squeezing than the conventional squeezing.

2 Noise budget

Fig. 3 displays the quantum noise budget for the QT squeezing, alongside the corresponding ETLF results for conventional squeezing.

Vacuum fields are introduced into the beam path by each loss source, and their total contribution is obtained by integrating the fields from the same loss point. Four optical losses have been accounted for, including (1) 4% injection loss that considers losses in the OPA cavity and Faraday isolator; (2) A loss of 45ppm assumed for the round-trip of light in the arm, as discussed in Section 1.2. (3) A loss of 1000ppm is assumed for the signal extraction mirror, the central beam splitter, and the imperfections of the Michelson interferometer, included in the overall SEC loss. (4) A 3% loss in readout due to the combined losses in the Faraday isolator, output mode cleaner, and inefficiency of the photo-detector. Losses from any source result in uncorrelated vacuum noise in the beam path that reduces the level of squeezing and correlation between EPR-entangled photons.

We evaluated three types of phase noise via root-mean-square (RMS) values in our analysis: (1) 10 milliradians of squeezer phase noise, which indicates the relative phase noise between the squeezer and the primary laser. (2) 10 mrad of local oscillator RMS phase uncertainty, which indicates the relative phase fluctuations between the local oscillator and the primary laser. (3) One picometer of SEC RMS length variations, which refers to the fluctuations in the optical length of the signal extraction cavity. These imperfections do not introduce any uncorrelated vacuum noise, rather contaminate the output with the contribution from the quadrature of light orthogonal to the one measured, which should not appear in the detection.

As shown in Fig. 3, all noises induced by phase fluctuations are included in the anti-symmetric (AS) port vacuum. It will be a subject of further research to break down the phase noise into parameters termed dephasing, as exemplified in [6], to elucidate the specific impact of each phase noise.

References

[1] Buonanno, A., Chen, Y.: Scaling law in signal recycled laser-interferometer gravitational-wave detectors. Phys. Rev. D **67**, 062002 (2003) https://doi.org/10.1103/PhysRevD.67.062002

[2] Danilishin, S.L., Khalili, F.Y.: Quantum measurement theory in gravitational-wave detectors. Living Reviews in Relativity **15**(1) (2012) https://doi.org/10.12942/lrr-2012-5

[3] Hild, S., *et al.*: Sensitivity studies for third-generation gravitational wave observatories. Classical and Quantum Gravity **28**(9), 094013 (2011) https://doi.org/10.1088/0264-9381/28/9/094013

[4] Khalili, F.Y.: Optimal configurations of filter cavity in future gravitational-wave detectors. Phys. Rev. D **81**, 122002 (2010) https://doi.org/10.1103/PhysRevD.81.122002

[5] Kwee, P., Miller, J., Isogai, T., Barsotti, L., Evans, M.: Decoherence and degradation of squeezed states in quantum filter cavities. Phys. Rev. D **90**, 062006 (2014) https://doi.org/10.1103/PhysRevD.90.062006

[6] McCuller, L., *et al.*: LIGO's quantum response to squeezed states. Phys. Rev. D **104**, 062006 (2021) https://doi.org/10.1103/PhysRevD.104.062006